Bulletin of the Earthquake
Research Institute
Vol. 42 (1964), pp. 491-514

25. *Deformation and Fracture of Rocks under Confining Pressure (1) Compression Tests on Dry Rock Sample.*

By Kiyoo Mogi,

Earthquake Research Institute.

(Read Feb. 25, 1964.—Received July 30, 1964.)

Abstract

Experimental study of the mechanical properties of rocks under high pressure and temperature is very helpful for making clear the mechanical behavior of the earth's crust and various phenomena originating from the earth's crust. Although much experimental work has been made, available data is still insufficient for a general discussion of the behavior of the various rocks from the geophysical point of view. In this series of experimental work, the effect of confining pressure on the deformation and fracture of different types of rocks are systematically investigated.

In this paper, the results of triaxial compression tests on twelve dry rocks, including diorite, granite, andesite, trachyte, tuff, sandstone and marble, are described. The confining pressure ranges from 1 to 1500 atmospheres. The stress-strain curves and curves for the breaking or yielding strength and the degree of the strain hardening as functions of confining pressure are given for each rock. The compact igneous rocks are very brittle and their breaking strength increases with the confining pressure. The sedimentary rocks and the porous igneous rocks become remarkably ductile under the moderate confining pressure. The extremely porous rocks behave as clastic materials under the influence of pressure.

1. Introduction

The experimental study of the mechanical behavior of rocks under high confining pressure and high temperature has been conducted by many investigators[1)-10)]. These laboratory experiments have provided

1) F. D. Adams and J. T. Nicolson, *Roy. Soc. London Philos. Trans.*, **A, 195** (1901), 363-401.

2) T. von Karman, *Zeit. des Ver. Deut. Ing.*, **55** (1911), 1749-1757.

3) D. T. Griggs, *Jour. Geol.*, **44** (1936), 541-577.

some important clues for investigations of various mechanical phenomena in the earth's crust and mantle, such as earthquakes and the crustal deformations. However, these experimental results are not always sufficient for application to many geophysical problems. The effect of confining pressure also does not seem to have been completely established for different types of rocks.

The most remarkable effects of the confining pressure are the increase of the strength and ductility of rocks. According to much experimental work, the breaking strength of very brittle rocks increases linearly with the confining pressure[11]. This experimental relation has also been explained on the modified Griffith theory by Brace[12]. However, in the brittle fracture strength of some rocks and in the yield strength, the relation between the strength and the confining pressure is different from the above-mentioned linear relation and a generalized relation including such cases has not been established. For a quantitative discussion of this problem, the present available data does not seem to be sufficient. That is, a large part of the tested rocks is carbonate rocks and the data on silicate rocks which are most important from the geophysical stand point are very few. Therefore, for a quantitative discussion of the pressure effect in the earth's crust, it is necessary to obtain more data on the different types of rocks. This paper is a preliminary report of the experiments for this purpose. An approximate relation between the strength and the pressure will be discussed in a next paper from the present available data reported by many investigators, including the data in this paper.

As mentioned above, the ductility of rocks increases with the confining pressure. Most rocks are exceedingly brittle under atmospheric pressure, but some rocks sustain a large amount of flowage without fracture under high confining pressure. This brittle-ductile transition is an interesting problem from the seismological point of view, as

4) E. C. ROBERTSON, *Bull. Geol. Soc. America*, **66** (1955), 1275-1314.

5) J. HANDIN and R. V. HARGER JR., *Bull. Assoc. Petrol. Geologists*, **41** (1957), 1-50.

6) J. HANDIN and R. V. HARGER JR., *Bull. Assoc. Petrol. Geologists*, **42** (1958), 2892-2934.

7) M. S. PATERSON, *Bull. Geol. Soc. America*, **69** (1958), 465-476.

8) D. GRIGGS and J. HANDIN, *Geol. Soc. America, Memoir* **79** (1960), 1-382.

9) S. MATSUSHIMA, *Disaster Research Inst. Bull.*, No. 36 (1960), 1-9.

10) W. F. BRACE, *Preprint of papers in International Conference on State of Stress in the Earth's Crust* (1963), 2.5-2.103.

11) E. C. ROBERTSON, *loc. cit.* 4).

12) W. F. BRACE, *loc. cit.* 10).

discussed by some investigators[13][14]. It has been widely believed among seismologists that earthquakes may be caused by brittle fracture of the earth's materials. According to the previous experiments, some rocks become remarkably ductile under environmental conditions at some depths in the earth's crust and the occurrence of earthquakes is impossible in the ductile state. It is very important to know the conditions of the brittle-ductile transition of various rocks.

The increase in ductility or the brittle-ductile transition has been studied by many investigators and the experimental work on Solenhofen limestone by Heard[15] is a very systematic one which has been carried out at elevated pressures and temperatures. However, the process of the brittle-to-ductile transition under the high confining pressure may be different in different types of rocks. The previous data does not cover the various rock types and they are also insufficient for general discussion of the transition process from brittle to ductile behavior in the earth's crust.

In this series of experimental study, the effects of confining pressure, especially the generalized strength-pressure relation and the process of the brittle-to-ductile transition, are systematically investigated on the basis of the experiments on different types of rocks. These two problems have a close connection with each other and so they should be discussed simultaneously, as seen in the next paper[16].

2. Experimental procedure

The strength of rocks is remarkably affected by various factors: the confining pressure, the temperature, the interstitial fluid pressure, the strain rate, etc. In this experiment, twelve dry rocks in Japan including various rock types were tested at room temperature by a conventional triaxial compression method. The samples of rocks were obtained from quarries in various districts in Japan. The test specimens were cylinders of 31 mm diameter and 62 mm height, the height-diameter ratio of 2.0. During testing the specimens were jacketed with soft rubber of 0.3 mm wall thickness and thin polyvinyl chloride sheet attached to the steel end pieces. This jacket prevents penetration of the pressure fluid and it gives no effect to the stress value of test specimens.

13) E. OROWAN, *Geol. Soc. America, Memoir* **79** (1960), 323-345.
14) D. GRIGGS and J. HANDIN, *Geol. Soc. America, Memoir* **79** (1960), 347-364.
15) H. C. HEARD, *Geol. Soc. America, Memoir* **79** (1960), 193-226.
16) K. MOGI, in preparation.

The testing apparatus is illustrated in Fig. 1. The pressure vessel was mounted between the platens of a hydraulic compression testing machine and the axial compression was applied by this testing machine. The confining pressure is supplied by another hydraulic pump which supplies the maximum pressure 3000 bar. The value of the pressure was indicated by a Boudom gauge. The maximum confining pressure applied in the present experiment was 1500 bar. The axial load was measured by a load cell of strain gauge type situated between the steel end piece of the test specimen and the inner bottom of the pressure vessel. This measurement is suitable for avoiding the error from the friction between the pressure vessel and a piston rod for axial loading.

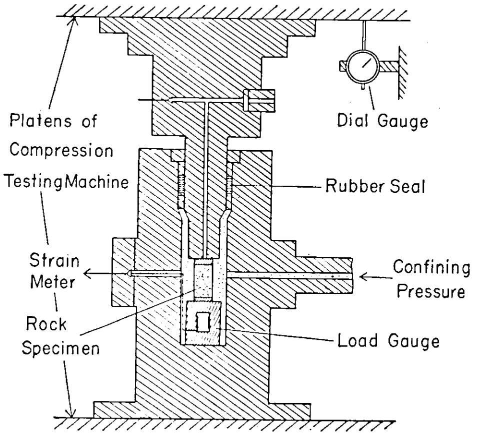

Fig. 1. Triaxial testing apparatus.

The strains were obtained from readings of a dial gauge placed between the platens of the testing machine. The reading of a dial gauge is 1/100 mm in accuracy. The dial gauge readings include the elastic strain in the apparatus. This strain can be measured from the tests on a steel piece of known elastic properties, and was reduced from the dial gauge readings. For hard rocks, this correction is considerably large.

The tests were made at nearly constant strain rate of one percent per 5 min. The differential stress was reduced to zero after about 5 percent deformation, for the purpose of investigating the stress-strain relation of remarkably strained rocks. The load and the strain readings were taken with interrupting the straining.

3. Experimental results

Compression stress-strain curves for different values of the confining pressure were obtained, as shown in Figs. 2~13. In this paper, the stress is quoted as the maximum difference of principal stresses, which is equal to twice the maximum shear stress. In all cases, the stress calculation is based on the initial cross-sectional area. Similarly the

Table 1. Summary of experiments.

Rock	No.	Confining pressure (kg/cm²)	Breaking or yield strength (kg/cm²)	Differential stress at 5 percent strain (kg/cm²)	Behavior	Angle of fracture
Ukigane diorite	111	1	1.88		brittle	
	112	400	4.45		brittle	25°
	113	700	5.49		brittle	26°
	114	1000	6.40		brittle	28°
Inada granite	121	1	1.44		brittle	
	122	350	5.22		brittle	23°
	123	500	5.96		brittle	20°
	124	1000	7.40		brittle	22°
Shirochōba andesite	131	1	1.11		brittle	
	132	350	2.35	1.75	brittle	30°
	133	500	3.20	2.65	transitional	35°
	134	1000	3.20			
	135	1500	4.00	4.10	ductile	40°
Honkomatsu andesite	141	1	0.75		brittle	
	142	500	1.00	1.44	ductile	
	143	1225	2.03	2.98	ductile	
	144	1475	2.23	3.23	ductile	
Tatsuyama tuff	151	1	0.96		brittle	
	152	500	2.22	1.49	brittle	30°
	153	1000	2.77	3.14	ductile	33°
	154	1500	2.77	4.24	ductile	30°
Mizuho trachyte	161	1	0.74		brittle	27°
	162	325	1.80		brittle	32°
	163	500	1.76	1.48	ductile	34°
	164	750	2.16	2.10	ductile	38°
	165	1000	2.16	2.22	ductile	40°
	166	1500	2.51	2.91	ductile	40°
Yamaguchi fine grained marble	171	1	0.68		brittle	
	172	300	1.53	1.42	ductile	28°
	173	500	1.77	1.88	ductile	30°
	174	1000		2.74	ductile	
	175	1500	2.32	3.18	ductile	

(to be continued)

Table 1. Summary of experiments (continued).

Rock	No.	Confining pressure (kg/cm^2)	Breaking or yield strength (kg/cm^2)	Differential stress at 5 percent strain (kg/cm^2)	Behavior	Angle of fracture
Mito medium grained marble	181	1	0.75		brittle	
	182	350	1.57		ductile	
	183	500	1.76		ductile	
	184	750	1.97	2.3	ductile	
	185	1500	2.26	3.2	ductile	
Yamaguchi coarse grained marble	191	1	0.50		brittle	
	192	350	0.93	1.24	ductile	
	193	500	(1.61)	1.86	ductile	
	194	750	0.95	2.10	ductile	
	195	1500	1.09	2.56	ductile	
Ao-ishi tuff	201	1	0.46*		brittle	
	202	350	0.53*	0.64	ductile	
	203	500	0.39*	0.65	ductile	
	204	1000	0.24*	0.97	ductile	
	205	1500	0.20*	1.34	ductile	
Ooya-ishi tuff	211	1	0.112*		brittle	
	212	500	0.095*	0.31	ductile	
	213	1000	0.095*	0.60	ductile	
	214	1500	0.017*	0.87	ductile	
Tako-ishi sandstone	221	1	0.20*		brittle	
	222	350	0.11*	0.28	ductile	
	223	500	0.06*	0.31	ductile	
	224	750	0.13*	0.49	ductile	
	225	1500	0.50*	1.48	ductile	

*) Differential stress at 1 percent strain.

strain is an average value of the specimen. From the stress-strain relation, the breaking strength, the yield strength and the maximum differential stress at 5 percent strain were obtained. The yield stress is the stress at the knee of the stress-strain curve. It is frequently indefinite because of the lack of a marked break in the curve. When the initial part of the stress-strain curve is nearly linear, the yield stress is defined as the stress at which the departure from linearity of a stress-strain curve is 0.2 percent strain.

In this paper, the difinition of the brittle and ductile behavior is obtained on the basis of the stress-strain relation. The brittle behavior is characterized by a sudden change of slope in the stress-strain curve at the yield point followed by a complete loss of cohesion or a remarkable drop in differential stress. The ductile behavior is by the deformation without any remarkable downward breaks in slope after the yield point.

The relation between the strength and the confining pressure in each rock is shown in Fig. 14. In this figure the breaking strength is shown by large closed circles, the yield strength by small closed circles, and the stress at 5 percent strain by open circles. The slope of the stress-strain curve after the yielding indicates the degree of the strain hardening. Here, the H value was taken as the measure of the strain hardening, as

$$H=\frac{\theta}{\sigma_m}\times 100\,(\%)\,,$$

where θ is the mean slope (kg/cm^2/1 percent strain) of the stress-strain curve between 2 and 5 percent strain and σ_m the maximum stress difference at the mean strain (3.5 percent strain). The relation between the H value and the confining pressure is shown in the same figures. The results of experiments are summarized in Table 1.

1. *Ukigane diorite*

Compression tests were made at 1, 300, 700, and 1000 bar confining pressure. This rock is very brittle at the tested confining pressures. The breaking strength increases remarkably with the confining pressure. The ultimate strain also increases with the pressure, but it does not exceed 2 percent strain. The test specimens fractured on steep shear surface inclined at 25° (400 bar), 26° (700 bar), and 28° (1000 bar) to a cylinder axis. The angle of fracture plane slightly increases with the confining pressure. The fracture angle predicted from the Mohr envelope is 22.5° (400 bar), 25.5° (700 bar), and 27.5° (1000 bar). The agreement of the observed angle and the calculated angle is very good.

2. *Inada granite*

The stress-strain curves are shown in Fig. 3. Inada granite is still very brittle at 1000 bar. At all pressures the specimen fractured with a loud detonation. The breaking strength increases more remarkably with the pressure as compared with the diorite. At atmospheric pressure, the fracture pattern is irregular. Under the pressure, the fracture is a shear type and the angle of shear surface is 23° (350 bar), 20° (500 bar), and 22° (1000 bar). The angle of fracture predicted from the Mohr envelope is 20.5° (350 bar), 25° (500 bar), and 28° (1000 bar). The agreement of the observation and the calculation is not so good. In this rock, the fracture plane is irregular to some degree, so the accuracy of angle measurement is low. The fracture angle of this rock is smaller than that of the diorite both in observed values and the predicted values.

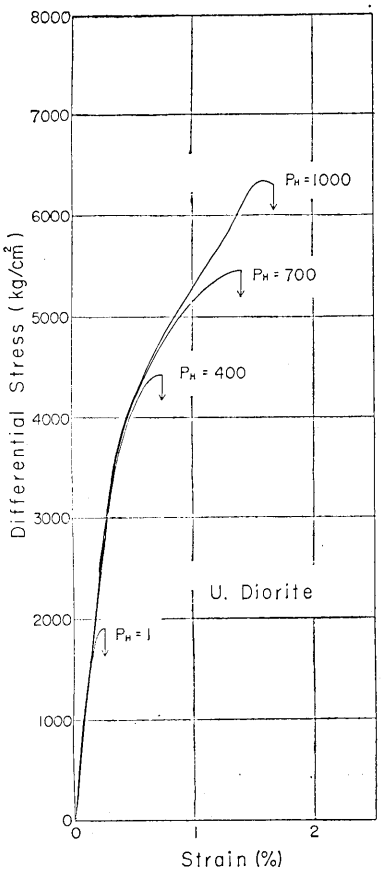

Fig. 2. Ukigane diorite.

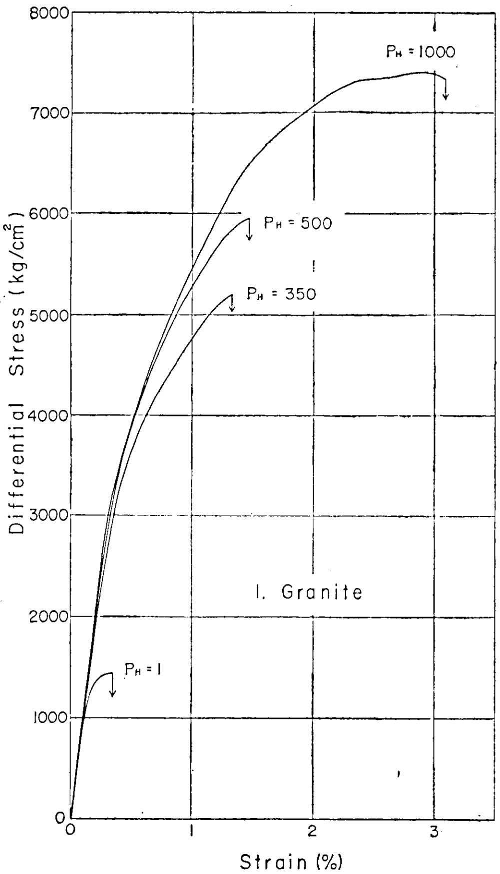

Fig. 3. Inada granite.

Figs. 2-3. Stress-strain curves for various rocks, tested in compression at room temperature. Confining pressures in atmospheres given for each curve.

3. *Shirochōba andesite*

The tests were made at 1, 350, 500, 1000, and 1500 bar. At atmospheric pressure, Shirochōba andesite is considerably brittle. At the confining pressure 350 bar, the differential stress decreases remarkably after a maximum value. In this case, if the axial stress is constantly maintained at the maximum value the increase of strain may be accelerated and the breaking fracture expected. Consequently, the

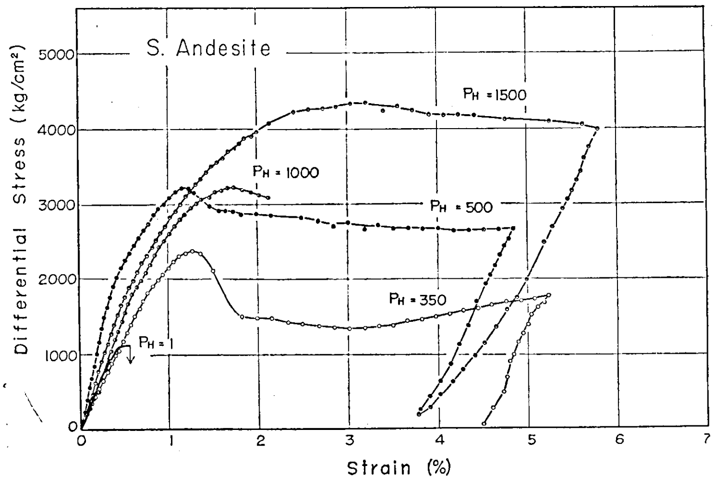

Fig. 4. Shirochōba andesite.

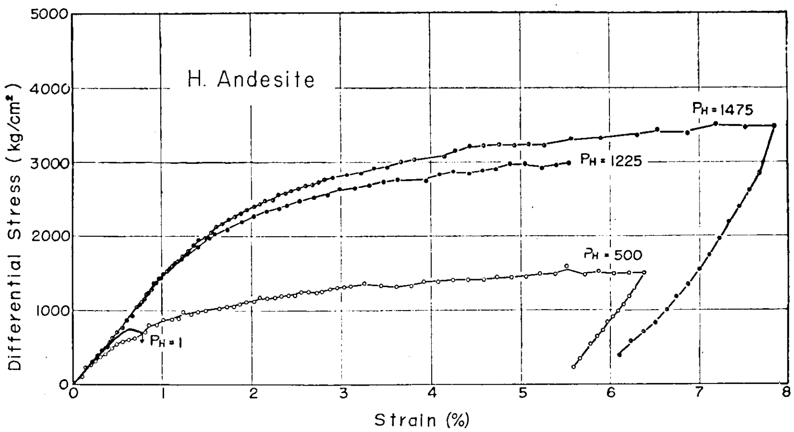

Fig. 5. Honkomatsu andesite.

Figs. 4-5. Stress-strain curves for various rocks, tested in compression at room temperature. Confining pressures in atmospheres given for each curve.

case where the axial stress decreases remarkably is also taken to be brittle. The stress-strain curve at 500 bar also shows a slight drop in the differential stress after the yield point. This case is a transitional one from a brittle to a ductile state. Under higher confining pressure it is clearly ductile. In this rock, the slope of the initial part of the curve before the yield point is different in each experiment, the curves being slightly concave downward. This seems to be due to the inhomogeneity of the rocks. In every case, except for atmospheric condition, the shear fracture is observed, the angle of fracture plane being 30° (350 bar), 35° (500 bar), and 40° (1500 bar). At atmospheric pressure, the extension fracture takes place and the fracture pattern is complex. The predicted angle from the Mohr envelope is 23.5° (350 bar), 29° (500 bar), and 37.5° (1500 bar). The breaking strength and the yield strength increase considerably with the confining pressure.

4. *Honkomatsu andesite*

Honkomatsu andesite is more porous than Shirochōba. As seen in the stress-strain curve in Fig. 5, at 500 bar the rock becomes remarkably ductile and the fracture takes place at localized shear planes. Under higher pressure, small fractures are uniformly distributed in the specimen. Such uniform deformation is common in the ductile state. In this rock, the knee of the stress-strain curves corresponding to the yield point is not so clear and the stress gradually increases with the increase of deformation.

5. *Tatsuyama tuff*

The tests were made at 1, 500, 1000, and 1500 bar confining pressure. The stress-strain curves are shown in Fig. 6. The stress-strain curve at 500 bar indicates a peak at the yield point and the stress decreases remarkably with the increase of the strain. This case also is thought to be brittle. At 1000 bar, the rock becomes clearly ductile. In the brittle state the strength increases appreciably with the increase in pressure, but in the ductile state it is almost constant. The fracture pattern at atmospheric pressure is very irregular and that of 500 bar is a single shear fracture. Under higher pressure, several shear fracture planes cross each other. The observed angle of fracture plane is about 30° (500 bar), 33° (1000 bar), and 30° (1500 bar). The angle predicted from the Mohr envelope is 31° (500 bar), 39° (1000 bar), and 45° (1500 bar). In this case, the H value, the degree of strain hardening, increases remarkably with the confining pressure, as shown in Fig. 14.

6. *Mizuho trachyte*

This rock is brittle at 325 bar and ductile at 500 bar. The yield stress continues to increase gradually with the increase in pressure. The increase of the H value with the confining pressure is not so remarkable (Fig. 14 (b)). At lower pressure, a single shear fracture takes place. Under higher pressure the crossed shear fracture appears, and at 1500 bar many micro-fractures are distributed uniformly in the specimen. The observed angle of fracture plane is about 27° (1 bar), 32° (325 bar), 34°

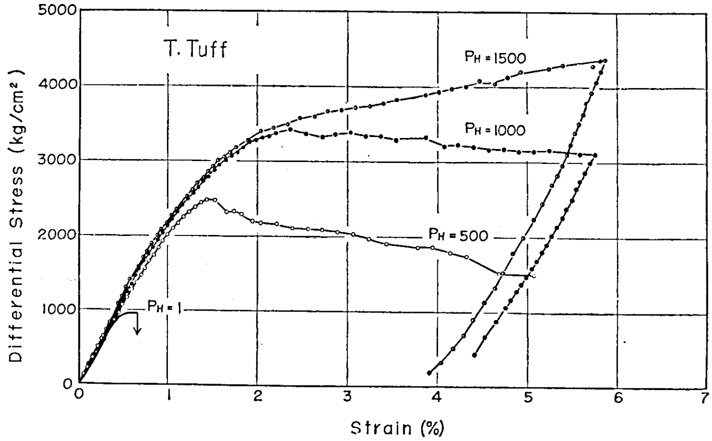

Fig. 6. Tatsuyama tuff.

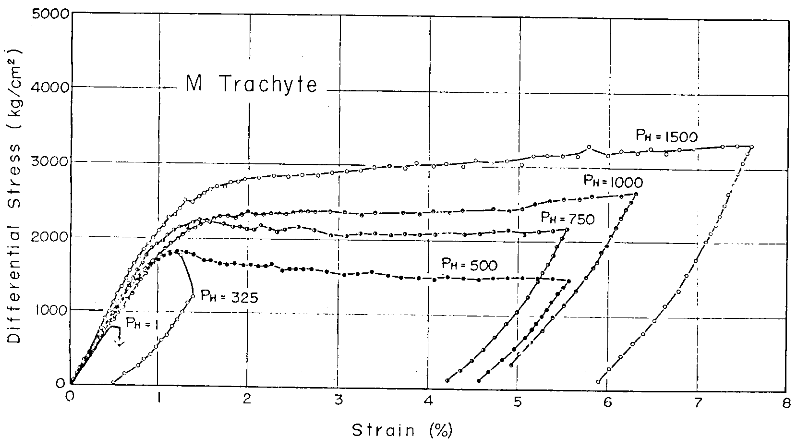

Fig. 7. Mizuho trachyte.

Figs. 6-7. Stress-strain curves for various rocks, tested in compression at room temperature. Confining pressures in atmospheres given for each curve.

(500 bar), 38° (750 bar), 40° (1000 bar), and 40° (1500 bar). The predicted angle from the Mohr envelope is 30° (1 bar), 30.5° (325 bar), 31° (500 bar), 32.5° (750 bar), 45° (1000 bar), and 45° (1500 bar). The agreement is well within the experimental accuracy.

7. *Yamaguchi fine grained marble, Mito medium grained marble, and Yamaguchi coarse grained marble.*

The above are all homogeneous white marbles. The stress-strain curves in Figs. 8, 9, and 10 are similar to those of carbonate rocks reported by many investigators. The experimental curves of the fine

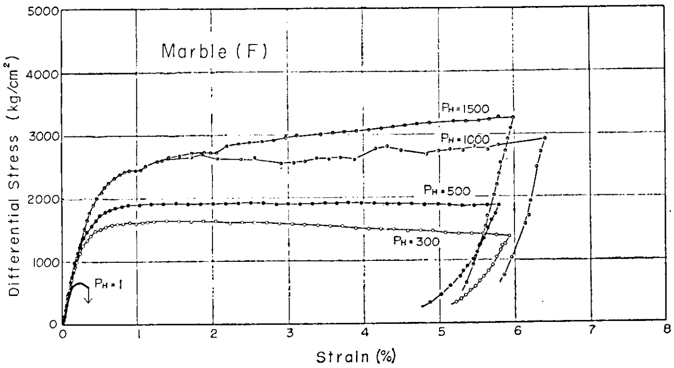

Fig. 8. Yamaguchi marble (fine grain).

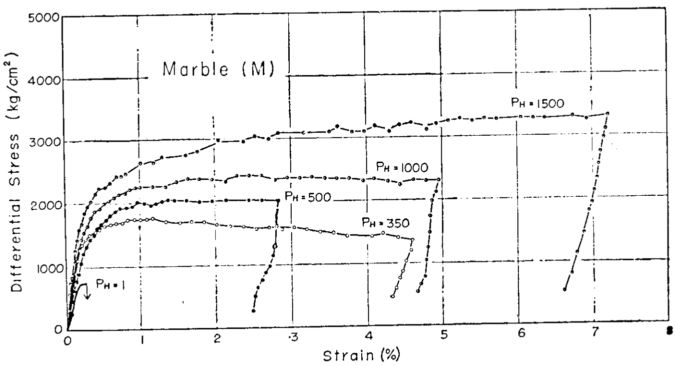

F. 9. Mito marble (medium grain).

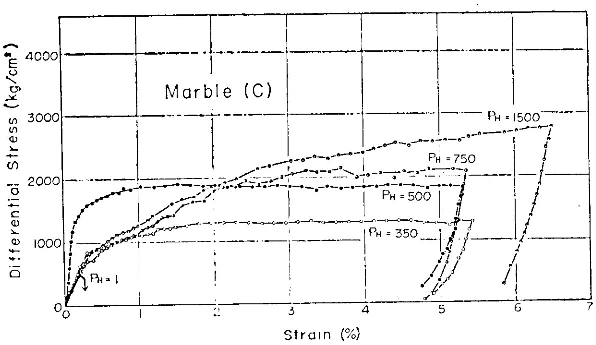

Fig. 10. Yamaguchi marble (coarse grain).

Figs. 8-10. Stress-strain curves for various rocks, tested in compression at room temperature. Confining pressures in atmospheres given for each curve.

grained marble coincide well while those of coarse grained marble deviate considerably from each other. These rocks become remarkably ductile at lower pressure and the degree of strain hardening (H) also increases with the confining pressure. The shear faults appear under lower pressure and the deformation under higher pressure is very homogeneous. The strength of the coarse grained marble is lower than

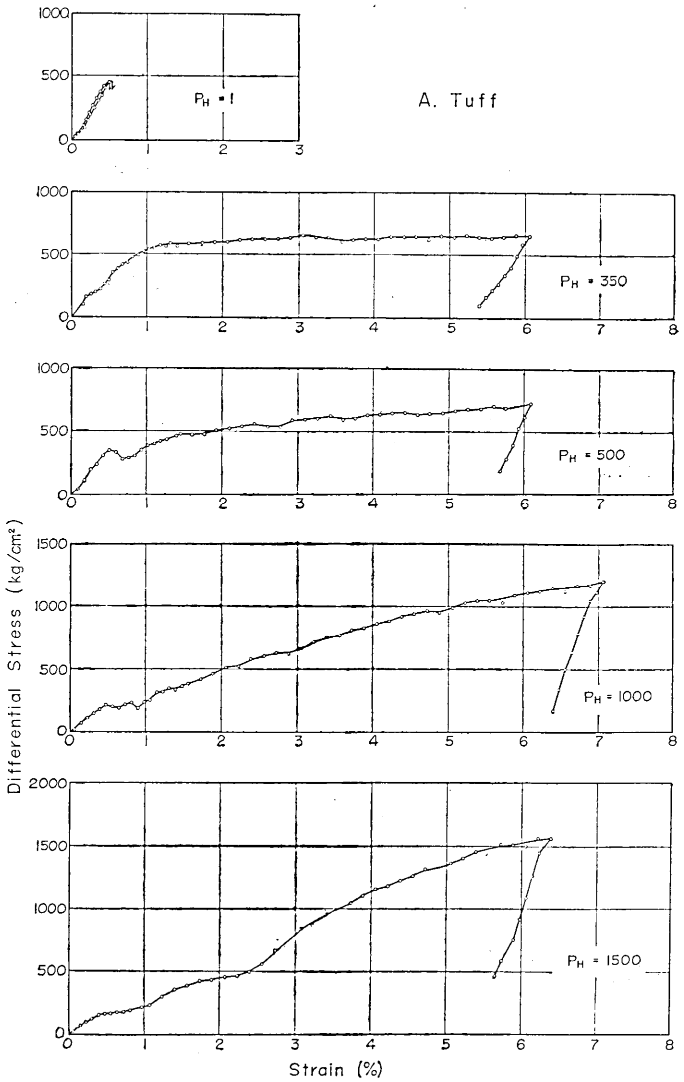

Fig. 11. Stress-strain curves of Ao-ishi tuff, tested in compression at room temperature. Confining pressures in atmospheres given for each curve.

that of fine grained marble, as discussed by Brace.[17)]

8. *Ao-ishi tuff* and *Ooya-ishi tuff*

These rocks are very porous with very low strength. The stress-strain curves of Ao-ishi are shown in Fig. 11. At 350 bar confining pressure, this rock is remarkably ductile and the strength is slightly higher than that at atmospheric pressure. However, under higher pres-

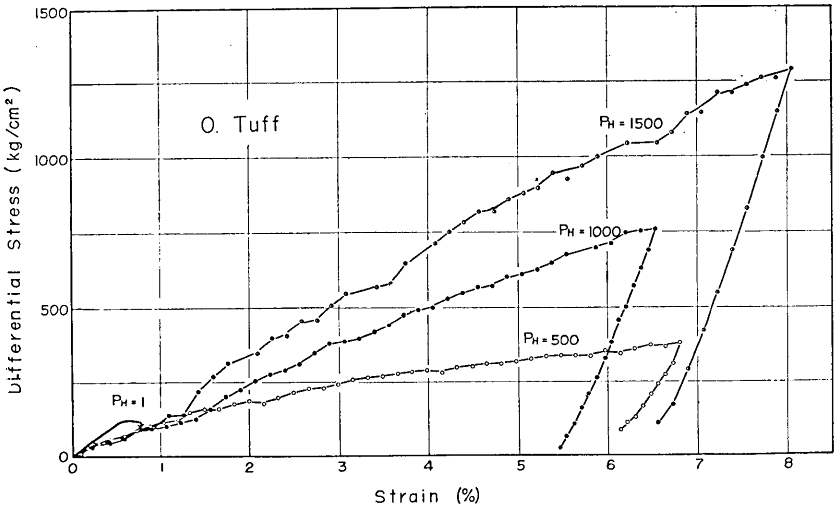

Fig. 12. Ooya-ishi tuff.

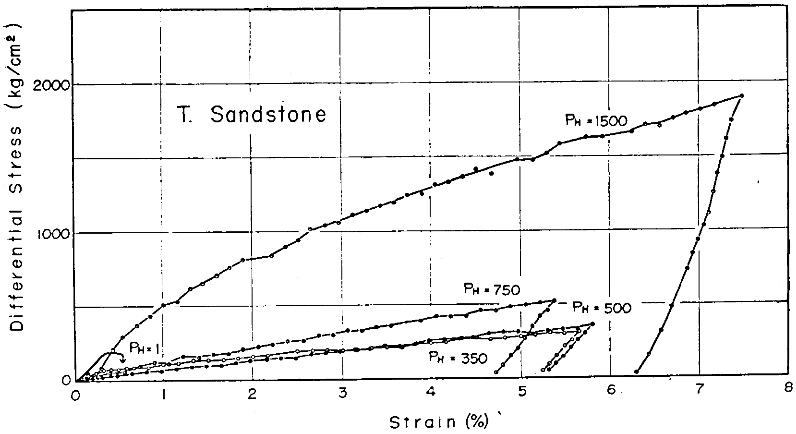

Fig. 13. Tako-ishi sandstone.

Figs. 12-13. Stress-strain curves for various rocks, tested in compression at room temperature. Confining pressures in atmospheres given in each curve.

17) W. F. BRACE, *Penn. State Univ. Mineral Expt. Sta. Bull.*, No. 76 (1961), 99-103.

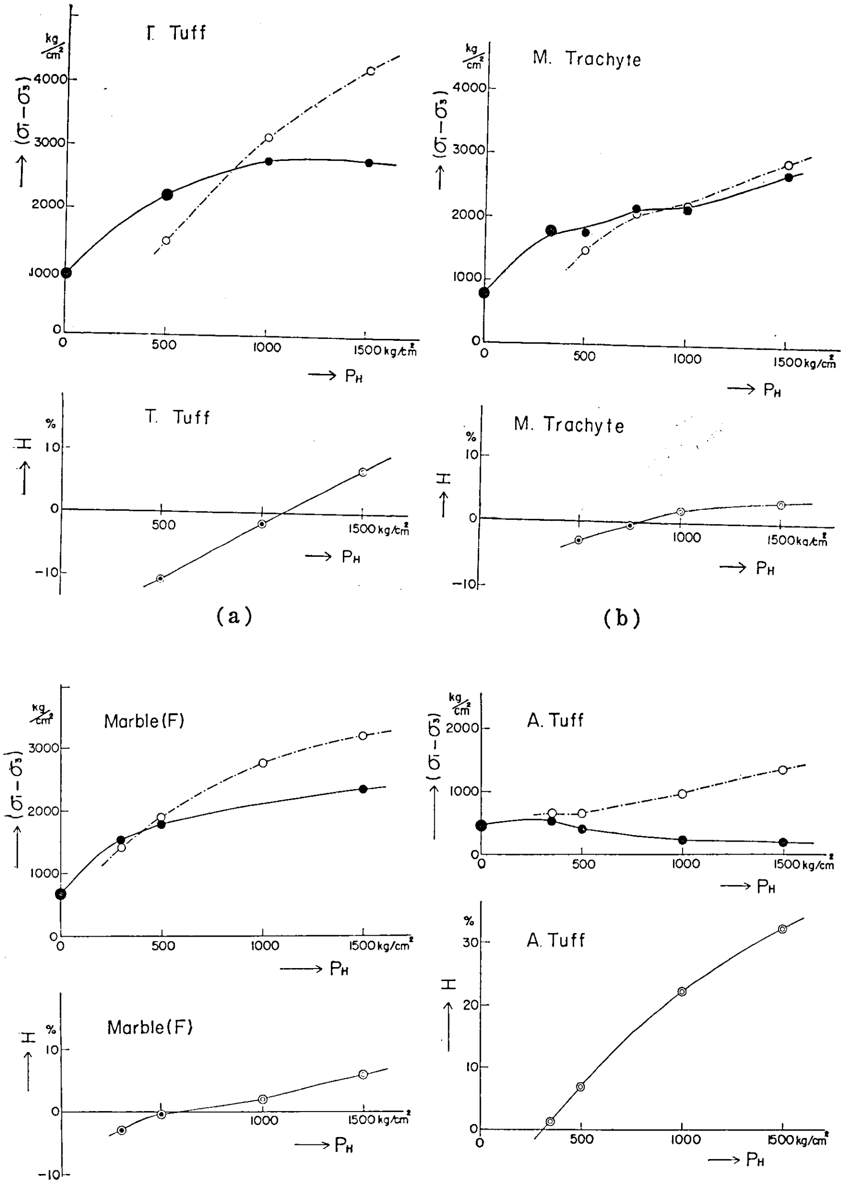

Figs. 14 (a)-(d). The strength and the degree of strain hardening (H) as functions of the confining pressure (P_H). Large closed circle: breaking strength, small closed circle: yield strength, open circle: differential stress at 5 percent strain.

sure the elastic limit decreases appreciably with the confining pressure. This is far different from the above-mentioned compact rocks. The pores are compacted by the applied pressure and so the mechanical framework is fractured by the hydrostatic pressure. Under higher pressure the stress increases remarkably with the large increase of deformation. This is very similar to the stress-strain relation in compacted clastic materials. As seen in Fig. 14 (c), the H value increases remarkably with the pressure. In this case, the clear fracture plane is not observed except for the atmospheric case and the deformation is very uniform.

Ooya-ishi is more porous and weaker than Ao-ishi. The stress-strain curves of Ooya-ishi are shown in Fig. 12. In this rock, the elastic limit is not clear except for the atmospheric case. This stress-strain curve is quite similar to that of clastic materials.

9. *Tako-ishi sandstone*

This rock is also very porous. The stress-strain curves shown in Fig. 13 are similar to that of porous tuff. At 1500 bar, the strain hardening is very remarkable. The deformation of specimen is very uniform and analogous to fluid materials.

4. Discussion

Relation between the strength and the confining pressure is summarized in Figs. 15 and 16. In compact rocks, the breaking strength in brittle state seems to increase remarkably with the confining pressure, as shown in many previous experiments. According to Tresca criterion on metals, the yield strength is independent of the confining pressure. In rocks, Tresca criterion is not always applicable, as indicated by Handin and Harger[18]. Although the increase in the strength is not so remarkable as in the brittle case, the yield strength in some rocks gradually increases with the pressure. However, the strength-pressure relation in very porous rocks is quite different from the above-mentioned relation in compact rocks. In this case, the rocks are fractured by the high hydrostatic pressure and so the strength decreases with the pressure. This difference between the compact rocks and the porous ones is not clear in the relation between the confining pressure and the stress difference at 5 percent strain. In this case, the stress difference increases more remarkably with the confining pressure.

According to Robertson[19], the mean pressure is more essential than

18) J. HANDIN and R. V. HARGER, *loc. cit.*, 5).
19) E. C. ROBERTSON, *loc. cit.*, 4).

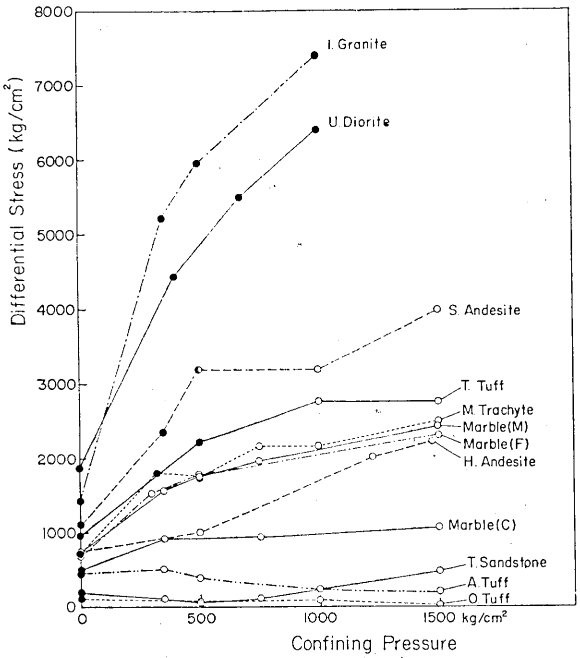

Fig. 15. Relation between the strength and the confining pressure. Closed circle: breaking strength, open circle: yield strength.

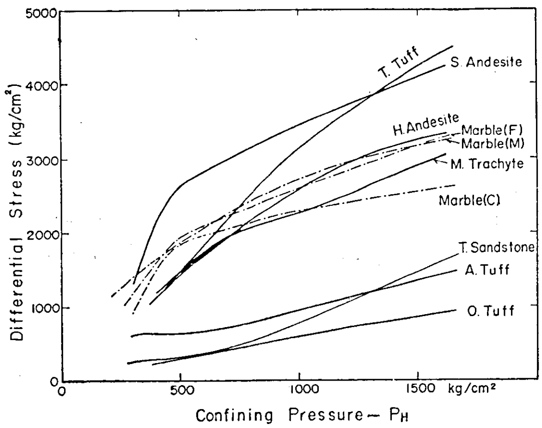

Fig. 16. Relation between the confining pressure and the stress at 5 percent strain.

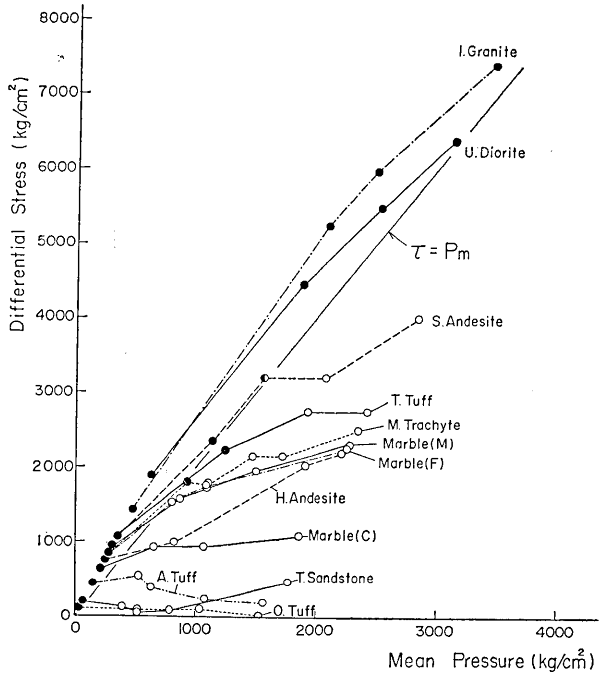

Fig. 17. Relation between the strength and the mean pressure. Closed circle: breaking strength, open circle: yield strength.

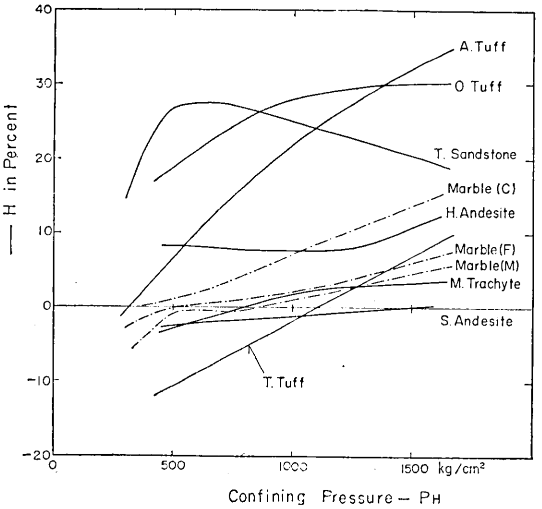

Fig. 18. Relation between the degree of strain hardening (H) and the confining pressure (P_H).

the confining pressure. Figure 17 shows the relation between the strength and the mean pressure. The line ($\tau = P_m$) indicates the relation proposed by Robertson as an approximate relation between the breaking

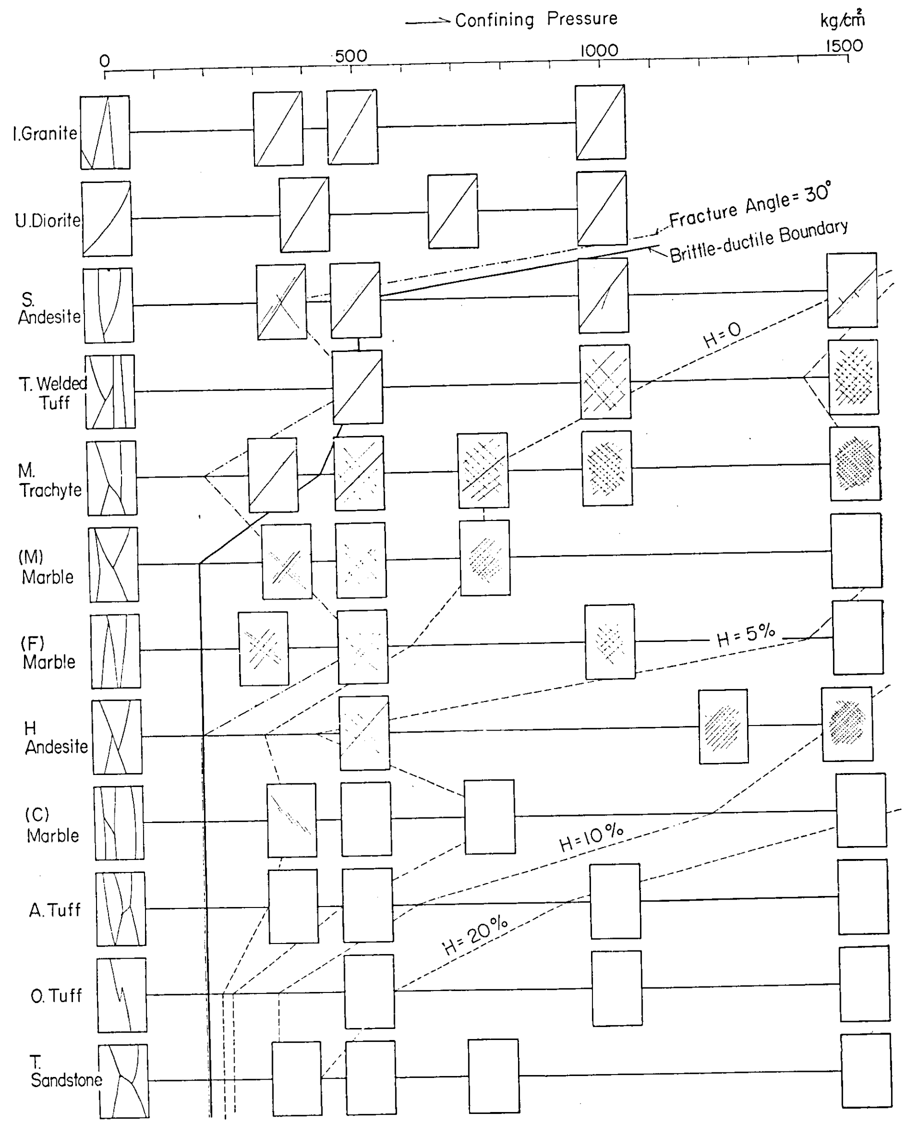

Fig. 19. Fracture patterns of various rocks for different values of confining pressure. Also, the boundary between the brittle state and the ductile state (solid line) and the lines of fracture angle 30° (chain line) and of various H values (broken line).

strength and the mean pressure. In Fig. 17, the brittle state is indicated by closed circles and the ductile state is by open circles. The brittle region and the ductile region seem to be divided by a boundary line irrespective of different types of rocks. This problem will be discussed in the next paper.

In Fig. 18, the relation between the degree of strain hardening and the pressure is shown. The H value increases with the confining pressure. The pressure at $H=0$ almost corresponds to the transition pressure from brittle fracture to ductile flow. The mechanism of strain hardening in the different types of rocks will be an interesting problem in the future.

The fracture patterns of various rocks for different values of pressure are schematically shown in Fig. 19. As mentioned above, such fracture patterns have a close relation with the stress-strain relation and the brittle or ductile behavior. In this figure, the boundary between the brittle state and the ductile state, and the lines of a value of fracture angle and of various H values are also shown. From these results, it is deduced that the degree of the brittleness of the tested rocks decreases systematically from the upper to the lower rock in this figure. The mechanical behavior of rocks may be specified by these various factors. The relation between the angle of fracture and the confining pressure is also shown in Fig. 20. The fracture angle increases with the confining pressure and the angle in the brittle state is smaller than that in the ductile state. However, the data is insufficient for further discussion.

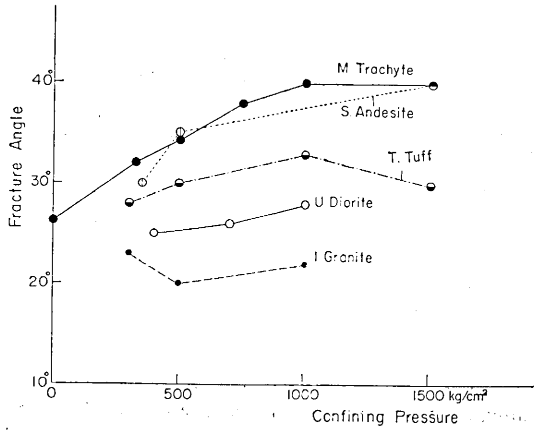

Fig. 20. Relation between the angle of fracture surface and the confining pressure.

Thus, in such rocks as sedimentary rocks and porous igneous rocks, the mechanical behavior is transferred from a brittle to a ductile type even under moderate pressure corresponding to the upper part of the earth's crust. At the elevated temperature, this transition from brittle fracture to ductile flow takes place at lower pressure. If these experimental results on dry rock samples are applied to the earth's layer of the above-mentioned types of rock, the brittle fracture cannot occur in the region where the overburden pressure is larger than the transition pressure from brittle fracture to ductile flow, and therefore earthquakes cannot take place in such regions. Seismicity at some regions seems to be explained by this mechanism. It has been noticed by Japanese seismologists that earthquakes do not occur at regions shallower than about 30 km directly under the Kantō plain, although they occur appreciably at deeper layers in this area and at shallow regions in the surrounding area. The sedimentary layer at the Kantō plain may be considerably thicker than that in the surrounding area. The seismic anomalous feature of the Kantō region may be understood as a ductile behavior of the layer in this region.

Table 2. Density and porosity of tested rocks.

Rock	Density	Porosity
U. Diorite	3.09	0.17%
I. Granite	2.61	0.42
S. Andesite	2.08	5.1
H. Andesite	2.23	9.9
T. Tuff	2.23	11.2
M. Trachyte	2.24	8.7
Marble (F)	2.62	0.34
Marble (M)	2.69	0.23
Marble (C)	2.48	0.15
A. Tuff	2.00	24
O. Tuff	1.45	30
T. Sandstone	1.94	15

5. Acknowledgements

The writer wishes to thank the staff of the Science and Engineering Research Laboratory, Waseda University, especially Drs. T. Yamazaki, I. Hayashi, and G. Endō for the use of the triaxial testing apparatus.

The writer also wishes to express thanks to Prof. T. Minakami for his valuable advice, to Dr. T. Matsuda for the petrographic description of tested rocks, and to Dr. N. Yamakawa for many valuable discussions. Financial aid for this experiment was granted partly by the Nomura Gakugeizaidan.

Appendix: Petrographic descriptions of rocks

Ukigane diorite—Ukigane is the trade name for the diorite quarried at Ononii-machi, Fukushima prefecture. The rock is a dark gray, very dense, medium grained rock. It is composed essentially of feldspar (mostly plagioclase), green hornblende, biotite, and a little quartz. [feldspar (up to 3 mm in diameter): 65 %, quartz (0.5 mm): 5 %, hornblende (1.5 mm): 20 %, biotite (1 mm): 10 %].

Inada granite—Inada is the trade name for the biotite granite quarried at Inada, Ibaragi prefecture. The rock is medium grained and light gray in colour. It contains K-feldspar, plagioclase, biotite and a small amount of muscovite. [K-feldspar (up to 4 mm in diameter): 40 %, biotite (0.5 mm): 10 %, quartz (3 mm): 30 %, plagioclase (1.5 mm): 20 %].

Mizuho trachyte—Mizuho is the trade name for the trachyte obtained from a quarry at Tomioka, Gumma prefecture. The rock is massive and light brownish gray in colour, with small spots of plagioclase phenocrysts. The groundmass is holocrystalline and consist mainly of plagioclase (oligoclase～andesine) and granulated (recrystallized?) quartz with small amounts of biotite, calcite and chlorite. [plagioclase (up to 0.5 mm in diameter): 70 %, quartz (0.1 mm): 1.5 %, biotite (0.1 mm): 7 %, calcite (1.5 mm): 5 %, chlorite (0.05 mm): 3 %].

Shirochōba andesite—Shirochōba is the trade name for the pyroxene andesite quarried at Manazuru, Kanagawa prefecture. The rock is light gray in colour. It is the hypersthene-augite andesite with phenocrysts of plagioclase, augite, hypersthene and magnetite. The groundmass is pilotaxitic in texture and contains plagioclase, augite and magnetite. [plagioclase (up to 1 mm in diameter): 85 %, augite (0.5 mm): 7 %, hypersthene (0.5 mm): 5 %, magnetite (0.15 mm): 3 %].

Honkomatsu andesite—Honkomatsu is the trade name for the augite andesite quarried at Manazuru, Kanagawa prefecture. The andesite is a compact, light gray rock with phenocrysts of plagioclase and augite. The plagioclase and augite in groundmass are various in size, fine- to coarse- grained. [plagioclase (up to 1 mm in diameter): 55 %, augite

(0.6 mm): 40 %, magnetite (0.04 mm): 5 %].

Tatsuyama tuff—Tatsuyama is the trade name for the dacite (welded?) pumice tuff quarried at Hōden, Hyōgo prefecture. The rock is a compact type, showing weak stratification. It is composed of devitrified pumice with phenocrysts of quartz. [quartz (up to 1.5 mm in diameter): 90 %, biotite (0.06 mm): 8 %, plagioclase (0.5 mm): 2 %].

Ao-ishi tuff—Ao-ishi is the trade name for the dacite pumice tuff quarried at Izu-Nagaoka, Shizuoka prefecture. The rock is compact, pale green and apparently massive, but a weak and fine lamination is recognizable on the polished surface. It is composed of altered quartz dacite pumice which contains albite, quartz, chlorite, calcite, epidote and pyrite. [chlorite: 50 %, quartz: 20 %, albite: 20 %, calcite: 6 %, epidote: 2 %, magnetite: 2 %].

Ooya-ishi tuff—Ooya-ishi is the trade name for the dacite pumice tuff obtained from a quarry at Ooya, Tochigi prefecture. The rock is a light gray type with greenish or brownish fragments of pumice. It is massive, but rugged. The rock is composed of slightly altered glassy pumice, containing phenocrysts of quartz, plagioclase, hornblende (rare) and biotite (rare). [glass: 30 %, chlorite: 30 %, quartz: 25 %, plagioclase: 10 %, magnetite: 3 %, hornblende: 1 %, biotite: 1 %].

Tako-ishi sandstone—Tako-ishi was obtained from a quarry at Yoshii, Gumma prefecture. The rock is massive, medium-grained and of a brownish light gray colour. It is composed mainly of angular quartz grains and shale fragments in rusty matrix. Grain size up to 0.5 mm.

Yamaguchi fine grained marble and coarse grained marble—The rocks are pure white calcite marbles quarried at Mine, Yamaguchi prefecture. The grain of the fine grained marble is up to 0.5 mm in diameter. The grain diameter of the coarse grained marble ranges from 1 mm to 8 mm.

Mito medium grained marble—This marble was obtained in a quarry at Oota, Ibaragi prefecture. It contains a little quartz (0.5~1 %).

25. 高封圧下の岩石の変形・破壊（第1報）乾いた試料の圧縮試験

地震研究所 茂 木 清 夫

地殻やマントルの力学的性質や地震の発生機構などの研究のために，地下深所に相当する高圧，高温のもとでの岩石の力学的諸性質を実験的に研究することが重要であると考えられる．このような立場からすでに多くの実験が行なわれ，いくつかの重要な成果が得られている．しかし，実験結果を実際の地殻の問題に適用するには，これまで研究されてきた岩石の種類が比較的限られていて，地殻を構成する各種岩石についての組織的な実験を集積する必要がある．このような立場から，各種主要岩石についての測定をはじめたが，本報告はその序報である．

今回は先ず本邦産の12種の岩石の試料約60について，高封圧のもとでの圧縮試験を行なつた．静水圧は油圧によつて最高1500気圧まで加えた．試料の内部に油が滲透するのを防ぐため，試料の表面をゴムおよびビニール膜で掩つた．軸圧は電気抵抗歪計による荷重計を用いて測定し，変形はダイヤルゲージでよみとつた．

圧力の増加と共に破壊強度および延性が著しく増大することは，すでにこれまでの報告に見られるものと同様である．ただ，岩石の種類，特にその空隙率のちがいによつて，その挙動が著しくちがつてくることが注目される．また，脆性から延性への遷移の仕方に規則性が見られるが，その詳しい考察は次の報告で行なう予定である．